

# Detection of SUSY in the stau–neutralino coannihilation region at the LHC

Richard Arnowitt<sup>a</sup>, Bhaskar Dutta<sup>a,\*</sup>, Teruki Kamon<sup>a</sup>, Nikolay Kolev<sup>b</sup>, David Toback<sup>b</sup>

<sup>a</sup> Department of Physics, Texas A&M University, College Station, TX 77843-4242, USA

<sup>b</sup> Department of Physics, University of Regina, Regina, SK S4S 0A2, Canada

Received 24 March 2006; received in revised form 12 May 2006; accepted 17 May 2006

Available online 16 June 2006

Editor: M. Cvetič

## Abstract

We study the feasibility of detecting the stau neutralino ( $\tilde{\tau}_1 - \tilde{\chi}_1^0$ ) coannihilation region at the LHC using tau ( $\tau$ ) leptons. The signal is characterized by multiple low energy  $\tau$  leptons from  $\tilde{\chi}_2^0 \rightarrow \tau \tilde{\tau}_1 \rightarrow \tau \tau \tilde{\chi}_1^0$  decays, where the  $\tilde{\tau}_1$  and  $\tilde{\chi}_1^0$  mass difference ( $\Delta M$ ) is constrained to be 5–15 GeV by current experimental bounds including the bound on the amount of neutralino cold dark matter. Within the framework of minimal supergravity models, we show that if hadronically decaying  $\tau$ 's can be identified with 50% efficiency for visible  $p_T > 20$  GeV the observation of such signals is possible in the final state of two  $\tau$  leptons plus large missing energy and two jets. With a gluino mass of 830 GeV the signal can be observed with as few as 3–10 fb<sup>-1</sup> of data (depending on the size of  $\Delta M$ ). Using a mass measurement of the  $\tau$  pairs with 10 fb<sup>-1</sup> we can determine  $\Delta M$  with a statistical uncertainty of 12% for  $\Delta M = 10$  GeV and an additional systematic uncertainty of 14% if the gluino mass has an uncertainty of 5%.

© 2006 Elsevier B.V. All rights reserved.

## 1. Introduction

The advent of supersymmetry (SUSY) has led to the construction of particle theory models linking a remarkably wide range of physical phenomena. While initially proposed on aesthetic grounds that nature should be symmetric between fermions and bosons, the fact that supersymmetry allows for the cancellation of the quadratic Higgs divergence allows the building of consistent models valid up to the grand unification (GUT) or Planck scales. The extension of supersymmetry to a local gauge theory, supergravity [1,2], led to the development of GUT models giving a description of physics from  $M_{\text{GUT}}$  down to the electroweak scale and incorporating the successes of the Standard Model (SM) [3–5]. Subsequently, LEP data experimentally confirmed the validity of the idea of SUSY grand unification. Further, an additional feature of SUSY is that models with  $R$ -parity invariance automatically give rise to a candidate, the lightest neutralino ( $\tilde{\chi}_1^0$ ), for the astronomically observed

cold dark matter (CDM) deeply linking particle physics with cosmology, and detailed theoretical calculations [6] confirm that GUT models can also achieve the experimentally observed amount of dark matter [7] in a natural way. A large number of experiments are now under way to try to detect SUSY dark matter in the Milky Way. Thus it is possible to construct models that encompass the full energy range of particle physics and simultaneously reach back into the early universe at times 10<sup>-7</sup> seconds after the Big Bang.

If supersymmetry ideas are correct, then the Large Hadron Collider (LHC) is expected to produce the  $\tilde{\chi}_1^0$  particles. Similarly, the large one ton dark matter detectors, currently under development, will cover a large amount of the allowed SUSY parameter space and may detect directly the Milky Way dark matter particles. Theory predicts that these two should be the same, and the question arises as to how one might verify this. The direct approach to this problem would involve having the dark matter detectors measure the nuclear differential cross section for the incident dark matter particle scattering from the detector atomic nuclei, and compare these with the differential cross sections occurring for the neutralinos produced in the LHC. Such measurements of course may be many years in the

\* Corresponding author.

E-mail address: [dutta@physics.tamu.edu](mailto:dutta@physics.tamu.edu) (B. Dutta).

future, and one would like to see if more immediate measurements might give strong indications for the equivalence of the astronomical and accelerator phenomena. To investigate this it is necessary to choose a SUSY model, and we consider in this Letter mSUGRA [3,4] (which has been used in many other LHC calculations).

The allowed mSUGRA parameter space, at present, has three distinct regions [6]: (i) the stau neutralino ( $\tilde{\tau}_1 - \tilde{\chi}_1^0$ ) coannihilation region where  $\tilde{\chi}_1^0$  is the lightest SUSY particle (LSP), (ii) the  $\tilde{\chi}_1^0$  having a larger higgsino component (focus point) and (iii) the scalar Higgs ( $A^0, H^0$ ) annihilation funnel ( $2M_{\tilde{\chi}_1^0} \simeq M_{A^0, H^0}$ ). These three regions have been selected out by the CDM constraint. (There still exists a bulk region where none of these above properties is observed, but this region is now very small due to the existence of other experimental bounds.) The distinction between the above regions cannot be observed in the dark matter direct detection experiments. To detect these regions, we are required to search for various signals such as neutrinos, gamma rays, positrons, and antiprotons expected from the annihilation of neutralinos and to combine them with the direct detection experiments [8]. It is therefore important to investigate whether the dark matter allowed regions can be observed at the LHC where the particles will be produced directly and their masses will be measured. The three dark matter allowed regions need very precise measurements at the colliders to confirm which is correct.

In this Letter we choose to work with the  $\tilde{\tau}_1 - \tilde{\chi}_1^0$  coannihilation region at the LHC. We note that many SUGRA models possess a coannihilation region and if the muon magnetic moment anomaly,  $a_\mu$ , maintains, it is the only allowed region for mSUGRA. Coannihilation is characterized by a mass difference ( $\Delta M$ ) between  $\tilde{\tau}_1$  and  $\tilde{\chi}_1^0$  of about 5–15 GeV in the allowed region. This narrow mass difference is necessary to allow the  $\tilde{\tau}_1$ 's to coannihilate in the early universe along with the  $\tilde{\chi}_1^0$ 's in order to produce the current amount of dark matter density of the universe. Thus if this striking near degeneracy between  $\tilde{\tau}_1$  and  $\tilde{\chi}_1^0$  is observed at the LHC, it would be a strong indirect indication that the  $\tilde{\chi}_1^0$  was the astronomical dark matter particle. The coannihilation region has a large extension for the gaugino mass  $m_{1/2}$ , up to 1–1.5 TeV, and can be explored at the LHC unless  $\tan\beta$  is very large.

We show here the feasibility of detecting a signal from the coannihilation region in the first few years of LHC running. The main difficulty, however, in probing this region is the small  $\Delta M$  value. Staus from  $\tilde{\tau}_1 \rightarrow \tau \tilde{\chi}_1^0$  decays generate signals with very low energy tau ( $\tau$ ) leptons and thus makes it difficult to discover this region at any collider due to the large size of the background events from the SM and SUSY processes. Signals with  $\tau$  leptons in the final states arising from the  $\tilde{\tau}_1, \tilde{\chi}_2^0$ , and  $\tilde{\chi}_1^\pm$  decays have been studied before in the context of the LHC for a large  $\Delta M$  value ( $\sim 50$  GeV) [9]. Detailed Monte Carlo (MC) studies have been performed to determine a subset of SUSY masses by fitting various mass distributions in SUSY particle decays [10], but at a pure generator level without any detector simulation such as effects by reconstruction, mis-identification, and the SM background. Those studies do not answer whether we can detect the coannihilation region at the LHC.

The primary feature of this region is that the branching fraction of the staus and gauginos to  $\tau$  leptons is very large, and that the kinematics of small  $\Delta M$  values produce these  $\tau$ 's with very low energy. Both conspire to make any analysis difficult as there can be very large backgrounds for low energy  $\tau$  final states. Previously we have shown a procedure to measure small  $\Delta M$  at an International Linear Collider (ILC) with an accuracy of about 10% for our benchmark points [11]. But the ILC is still in the proposal stage. Thus, it is important to see if the coannihilation signal can be observed at the LHC.

We describe here an experimental prescription for detecting SUSY signal in the coannihilation region and measuring small  $\Delta M$  at the LHC which provides a necessary condition to be in this region. We first discuss the available mSUGRA parameter space in Section 2 and the sparticle masses in this region. In Section 3 we detail a search for  $\tau$  pairs from  $\tilde{\chi}_2^0 \rightarrow \tau \tilde{\tau}_1 \rightarrow \tau \tau \tilde{\chi}_1^0$  decays and select events in the two  $\tau$  leptons plus large  $E_T$  jet(s) and large missing transverse energy ( $\cancel{E}_T$ ) final state. In particular, we motivate our selection criteria, describe the  $\tau\tau$  mass and counting observables that would provide consistency checks and other evidence, and indicate the amount of luminosity needed to establish a  $5\sigma$  significance. In this section it will become clear that a primary consideration for this analysis to have sensitivity is for the LHC detectors to have efficiency for  $\tau$ 's with  $p_T > 20$  GeV. In Section 4, we discuss a method of measuring  $\Delta M$  and show the potential accuracy. We conclude in Section 5.

## 2. mSUGRA model in the coannihilation region

The mSUGRA model depends upon four parameters in addition to those of the SM. They are  $m_0$ , the universal scalar soft breaking parameter at  $M_{\text{GUT}}$ ;  $m_{1/2}$ , the universal gaugino mass at  $M_{\text{GUT}}$ ;  $A_0$ , the universal cubic soft breaking mass at  $M_{\text{GUT}}$ ; and  $\tan\beta = \langle \hat{H}_1 \rangle / \langle \hat{H}_2 \rangle$  at the electroweak scale, where  $\hat{H}_1$  ( $\hat{H}_2$ ) gives rise to up-type (down-type) quark masses. The model parameters are already significantly constrained by different experimental results. Most important for limiting the parameter space are: (i) the light Higgs mass bound of  $M_{h^0} > 114$  GeV from LEP [12], (ii) the  $b \rightarrow s\gamma$  branching ratio bound of  $1.8 \times 10^{-4} < \mathcal{B}(b \rightarrow X_s \gamma) < 4.5 \times 10^{-4}$  (we assume here a relatively broad range, since there are theoretical errors in extracting the branching ratio from the data) [13], (iii) the  $2\sigma$  bound on the dark matter relic density:  $0.095 < \Omega_{\text{CDM}} h^2 < 0.129$  [7], (iv) the bound on the lightest chargino mass of  $M_{\tilde{\chi}_1^\pm} > 104$  GeV from LEP [14] and (v) the muon magnetic moment anomaly  $a_\mu$ , where one gets a  $2.7\sigma$  deviation from the SM from the experimental result [15–17]. Assuming the future data confirms the  $a_\mu$  anomaly, the combined effects of  $g_\mu - 2$  and  $M_{\tilde{\chi}_1^\pm} > 104$  GeV then only allows  $\mu > 0$ .

Fig. 1 shows the range of allowed  $\Delta M$  values in the coannihilation region as a function of  $m_{1/2}$  for  $\tan\beta = 40$ . We see that  $\Delta M$  is narrowly constrained and varies from 5–15 GeV. Because of the small  $\Delta M$  value,  $\tau$ 's from  $\tilde{\tau}_1 \rightarrow \tau \tilde{\chi}_1^0$  decays are expected to have low energy providing the characteristic feature of the coannihilation region. From here on, we assume

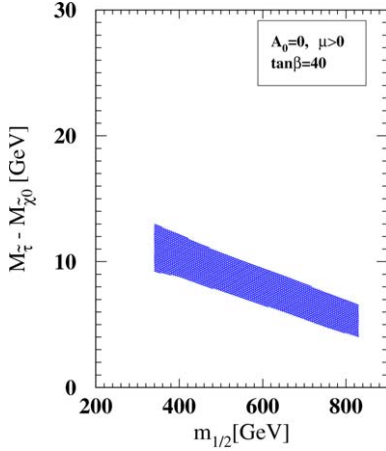


Fig. 1. The narrow  $\Delta M$  coannihilation band is plotted as a function of  $m_{1/2}$  for  $\tan\beta = 40$  with  $A_0 = 0$  and  $\mu > 0$ . The left end of the band is due to the  $b \rightarrow s\gamma$  branching ratio bound and the right end by  $a\mu < 11 \times 10^{-10}$ .

Table 1

Masses (in GeV) of SUSY particles in five representative scenarios for  $m_{1/2} = 360$  GeV,  $\tan\beta = 40$ ,  $\mu > 0$ , and  $A_0 = 0$ . These points satisfy all the existing experimental bounds on mSUGRA.  $M_{\tau\tau}^{\max}$  is the end point of the di-tau mass distribution from the  $\tilde{\chi}_2^0$  decays. The production cross section is nearly same for the five points and is 8.3 pb for  $m_0 = 215$  GeV

$m_0$	210	212	215	217	220
$\tilde{g}$	831	831	831	831	832
$\tilde{u}_L$	764	764	765	765	766
$\tilde{u}_R$	740	740	741	741	742
$\tilde{t}_2$	744	744	744	745	745
$\tilde{t}_1$	578	578	579	579	580
$\tilde{\tau}_2$	331	332	333	334	336
$\tilde{e}_L$	323	324	326	328	330
$\tilde{\chi}_2^0$	266	266	266	266	266
$\tilde{e}_R$	252	254	256	258	260
$\tilde{\tau}_1$	149.9	151.8	154.8	156.7	159.5
$\tilde{\chi}_1^0$	144.2	144.2	144.2	144.2	144.2
$\Delta M (\equiv M_{\tilde{\tau}_1} - M_{\tilde{\chi}_1^0})$	5.7	7.6	10.6	12.5	15.4
$M_{\tau\tau}^{\max}$	60.0	68.3	78.7	84.1	91.2

$m_{1/2} = 360$  GeV and  $\tan\beta = 40$  as a reference point and use it throughout the text unless otherwise noted. SUSY masses for five example those points are listed in Table 1 using ISAJET 7.63 [18].

### 3. Detecting a SUSY signal in the coannihilation region

Unlike at the ILC [11], it is very difficult to access direct  $\tilde{\tau}_1^+ \tilde{\tau}_1^-$  production at the LHC because of its small production cross section relative to the huge QCD backgrounds. Therefore, we will show that using copious  $\tilde{\chi}_2^0$  production and decay via  $\tilde{\chi}_2^0 \rightarrow \tau \tilde{\tau}_1 \rightarrow \tau \tau \tilde{\chi}_1^0$  a significant number of di-tau events can be observed with an effective observable. The end point of the mass distribution is calculated to be

$$M_{\tau\tau}^{\max} = M_{\tilde{\chi}_2^0} \sqrt{1 - \frac{M_{\tilde{\tau}_1}^2}{M_{\tilde{\chi}_2^0}^2}} \sqrt{1 - \frac{M_{\tilde{\chi}_1^0}^2}{M_{\tilde{\tau}_1}^2}}, \quad (1)$$

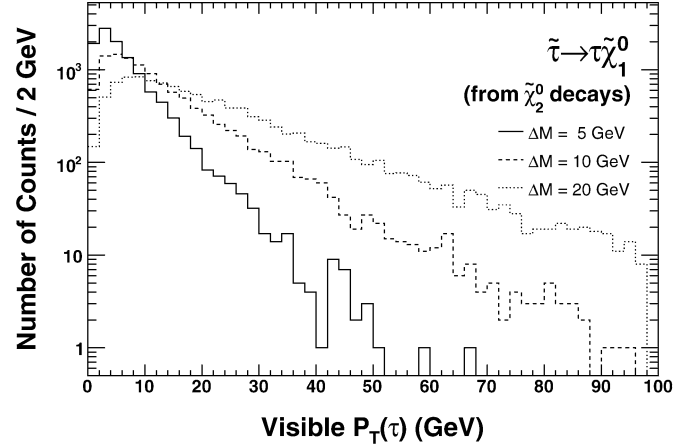


Fig. 2. The visible  $p_T$  distributions for hadronically decaying  $\tau$  leptons from  $\tilde{\tau}_1 \rightarrow \tau \tilde{\chi}_1^0$  where the  $\tilde{\tau}_1$ 's are required to be decays of  $\tilde{\chi}_2^0 \rightarrow \tau \tilde{\tau}_1$ . The curves show the results for  $\Delta M = 5, 10$ , and  $20$  GeV.

which corresponds to the case when the two  $\tau$ 's are back-to-back in the  $\tilde{\chi}_2^0$  rest frame. To reconstruct the mass as fully as possible we use hadronically decaying  $\tau$ 's ( $\tau_h$ 's). Despite the fact that the  $\tau$ 's lose energy to neutrinos, the di-tau mass distribution ( $M_{\tau\tau}^{\text{vis}}$ ) still provides a peak position ( $M_{\tau\tau}^{\text{peak}}$ ) that can be directly measured. The peak position is below  $M_{\tau\tau}^{\max}$  and  $M_{\tau\tau}^{\text{vis}}$  is effectively smeared. We next describe how to use these experimental features to detect the signal.

The primary SUSY production processes at the LHC are  $pp \rightarrow q\tilde{q}, \tilde{q}\tilde{q}, \tilde{g}\tilde{g}$ . In each case the decays proceed via  $\tilde{q} \rightarrow q'\tilde{\chi}_1^\pm$  or  $q\tilde{\chi}_2^0$  (or  $\tilde{q}_R \rightarrow q\tilde{\chi}_1^0$ );  $\tilde{g} \rightarrow q\tilde{q}'\tilde{\chi}_1^\pm$  or  $q\tilde{q}\tilde{\chi}_2^0$ ; and  $\tilde{g} \rightarrow \tilde{t}\tilde{t}_1$  or  $\tilde{b}\tilde{b}_1$  and their charge conjugate states, generally producing high  $E_T$  jets and gaugino pairs. We are most interested in events from  $\tilde{\chi}_1^0 \tilde{\chi}_2^0$ ,  $\tilde{\chi}_1^\pm \tilde{\chi}_2^0$ , or  $\tilde{\chi}_2^0 \tilde{\chi}_2^0$  pairs, where the  $\tilde{\chi}_1^0$  in the first case is directly from the  $\tilde{q}_R$  decay. The branching ratio of  $\tilde{\chi}_2^0 \rightarrow \tau \tilde{\tau}_1$  is about 97% for our parameter space and is dominant even for large  $m_{1/2}$  in the entire coannihilation region; the same is true for the  $\tilde{\chi}_1^\pm \rightarrow \nu \tilde{\tau}_1$  decay mode. (It should be noted that both  $\tilde{e}_R$  and  $\tilde{\mu}_R$  are lighter than  $\tilde{\chi}_2^0$  by about 10 GeV. However, the branching ratio for  $\tilde{\chi}_2^0 \rightarrow e\tilde{e}_R$  or  $\mu\tilde{\mu}_R$  is much less than 1%.) Since the stau decays via  $\tilde{\tau}_1 \rightarrow \tau \tilde{\chi}_1^0$ , we expect inclusive  $\tilde{\chi}_2^0$  events to include at least two  $\tau$  leptons plus large  $E_T$  jet(s) and large  $\cancel{E}_T$  (from the  $\tilde{\chi}_1^0$ ).

We consider two experimental scenarios. The first uses the  $\cancel{E}_T + \geq 2$  jet final state to reduce backgrounds and searches for the  $2\tau$ 's that arises from the decays of a  $\tilde{\chi}_2^0$ . In each candidate event, all di-tau pairs can then be searched for a mass peak as evidence of the  $\tilde{\chi}_2^0$  decay chain. The second option studies gaugino pairs ( $\tilde{\chi}_2^0 \tilde{\chi}_2^0$ ,  $\tilde{\chi}_1^\pm \tilde{\chi}_2^0$ ) and used  $3\tau$ 's to reduce backgrounds and  $\cancel{E}_T + \geq 1$  jet to regain acceptance. Both final states will be triggered by requiring large  $E_T$  jet(s) and large  $\cancel{E}_T$  and such a trigger will be available at both the ATLAS and the CMS experiments. We focus on the final event selection and report here on an analysis of the  $\cancel{E}_T + \geq 2$  jet +  $\geq 2\tau$  events using the ISAJET event generator and the ATLAS detector simulation ATLFAT [19]. The results of the  $3\tau$  analysis will be considered elsewhere [20].

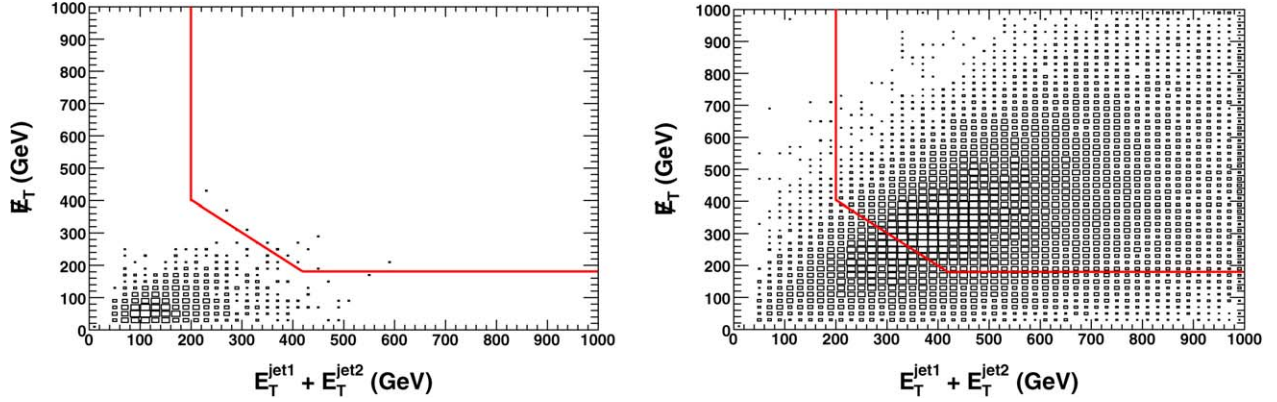


Fig. 3. Scatter plots of  $\cancel{E}_T$  vs  $E_T^{\text{jet1}} + E_T^{\text{jet2}}$  for  $t\bar{t}$  (left) and SUSY (right) events after requiring  $2\tau$ 's passing all ID and kinematic cuts in the final state. The SUSY events are for our reference point at  $M_{\tilde{g}} = 831$  GeV and  $\Delta M = 10.6$  GeV. We require  $E_T^{\text{jet1}} > 100$  GeV,  $E_T^{\text{jet2}} > 100$  GeV,  $\cancel{E}_T > 180$  GeV, and  $E_T^{\text{jet1}} + E_T^{\text{jet2}} + \cancel{E}_T > 600$  GeV to eliminate the top background.

To establish a signal in the coannihilation region we require (at least) (1) a  $5\sigma$  excess in the counting of  $\cancel{E}_T + 2 \text{ jet} + 2\tau$  events with  $M_{\tau\tau}^{\text{vis}}$  below  $M_{\tau\tau}^{\text{max}}$  and (2) the mass peak to be consistent with the expectations from  $\tilde{\chi}_2^0$  decays. The question then becomes whether such measurements are possible at the LHC. We begin by addressing the primary experimental issues: (a) the  $p_T$  spectrum of  $\tau$ 's from  $\tilde{\tau}_1 \rightarrow \tau \tilde{\chi}_1^0$  which is expected to be soft and (b) the ability to select the correct di-tau pairs.

We first examine the visible  $p_T$  ( $p_T^{\text{vis}}$ ) distribution of  $\tau_h$ 's from  $\tilde{\tau}_1 \rightarrow \tau \tilde{\chi}_1^0$  in  $\tilde{\chi}_2^0$  decays with  $\Delta M = 5, 10$ , and  $20$  GeV using ISAJET. As seen in Fig. 2, even with a small mass difference, the  $\tau$  is boosted in the cascade decay of the heavy squark and gluino making it potentially viable. One can already begin to see the importance of reconstructing the  $\tau$ 's with  $p_T^{\text{vis}} \gtrsim 20$  GeV. From here on, we assume that both the ATLAS and CMS detectors can reconstruct and identify  $\tau_h$ 's with  $p_T^{\text{vis}} > 20$  GeV. Assuming the taus are identifiable, we require two jets with  $E_T > 100$  GeV and  $\cancel{E}_T > 180$  GeV. These cuts should satisfy the  $\cancel{E}_T + \text{jets}$  trigger at ATLAS and CMS with high enough efficiency that we further neglect trigger efficiency and bias effects.

Events are further selected by requiring at least two identified  $\tau_h$ 's with at least one  $\tau$  lepton with  $p_T^{\text{vis}} > 40$  GeV (from  $\tilde{\chi}_2^0 \rightarrow \tau \tilde{\tau}_1$ ) and one with  $p_T^{\text{vis}} > 20$  GeV (from  $\tilde{\tau}_1 \rightarrow \tau \tilde{\chi}_1^0$ ). At this point, the dominant background is expected to be from  $t\bar{t}$  pair production, where each  $t$  decays as  $t \rightarrow b\tau\nu$  and produces a final state of  $\cancel{E}_T + 2b + 2\tau$ . A correlation plot between  $\cancel{E}_T$  and  $E_T^{\text{jet1}} + E_T^{\text{jet2}}$  is shown in Fig. 3 for  $t\bar{t}$  and SUSY events. We choose  $E_T^{\text{jet1}} + E_T^{\text{jet2}} + \cancel{E}_T > 600$  GeV to further reduce the background.

For each candidate  $M_{\tau\tau}^{\text{vis}}$  is calculated for every pair of  $\tau$ 's in the event and categorized as opposite sign (OS) or like sign (LS). The mass distribution for LS pairs is subtracted from the distribution for OS pairs to extract  $\tilde{\chi}_2^0$  decays on a statistical basis. We first show the result in Fig. 4 where we have assumed the identification (ID) efficiency ( $\epsilon$ ) to be 100% and a probability that a jet is misidentified as  $\tau_h$  ( $f_{j \rightarrow \tau}$ ) to be 0%. We see that the non- $\tilde{\chi}_2^0$  OS pairs are nicely canceled with the wrong LS combination pairs and that the OS–LS distribution is well

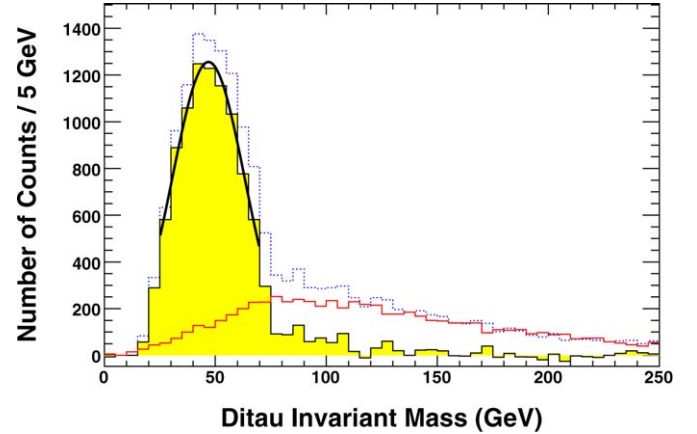


Fig. 4. The visible di-tau invariant mass ( $M_{\tau\tau}^{\text{vis}}$ ) distributions for all di-tau combinations in inclusive  $\cancel{E}_T + 2 \text{ jet} + 2\tau$  events in the coannihilation region ( $\Delta M = 10.6$  GeV; see Table 1) with  $\epsilon = 100\%$  and  $f_{j \rightarrow \tau} = 0\%$ . The luminosity of the SUSY sample is  $200 \text{ fb}^{-1}$ . The  $\tau$ 's are selected with  $p_T^{\text{vis}} > 20$  GeV but requiring at least one  $\tau$  lepton to have  $p_T^{\text{vis}} > 40$  GeV. The endpoint is consistent with the theoretical value at  $M_{\tau\tau}^{\text{max}} = 78.7$  GeV. The dashed and solid open histograms are for OS and LS pairs, respectively. The gray (or yellow) histogram is for OS–LS pairs and is well fitted to a Gaussian (solid line). The small excess between 80 and 150 GeV is mainly due to  $\tilde{\chi}_3^0(456 \text{ GeV}) \rightarrow \tau \tilde{\tau}_1, Z \tilde{\chi}_2^0, W^\pm \tilde{\chi}_1^\mp$  decays. (For interpretation of the references to color in this figure legend, the reader is referred to the web version of this Letter.)

fit to a Gaussian. While the expected maximum di-tau mass,  $M_{\tau\tau}^{\text{max}} = 78.7$  GeV, is consistent with Fig. 4 and easily determined, we believe a full detector simulation is required to show this in practice. We note for completeness that there is a small second excess between 80 and 150 GeV, which is mainly due to  $\tilde{\chi}_3^0(456 \text{ GeV}) \rightarrow \tau \tilde{\tau}_1, Z \tilde{\chi}_2^0, W^\pm \tilde{\chi}_1^\mp$  decays.

We next assume  $\epsilon = 50\%$  and  $f_{j \rightarrow \tau} = 1\%$ , based on the CDF measurement [21], and show that these results are not significantly affected by these experimental conditions except to quadruple the needed luminosity to establish a signal. Fig. 5 shows the  $M_{\tau\tau}^{\text{vis}}$  distributions for OS, LS, and OS–LS pairs for a hypothetical  $10 \text{ fb}^{-1}$  SUSY sample to allow visual confirmation of the peak taking into account statistical fluctuations. We see approximately 120 OS–LS pairs. The excess between 80 and



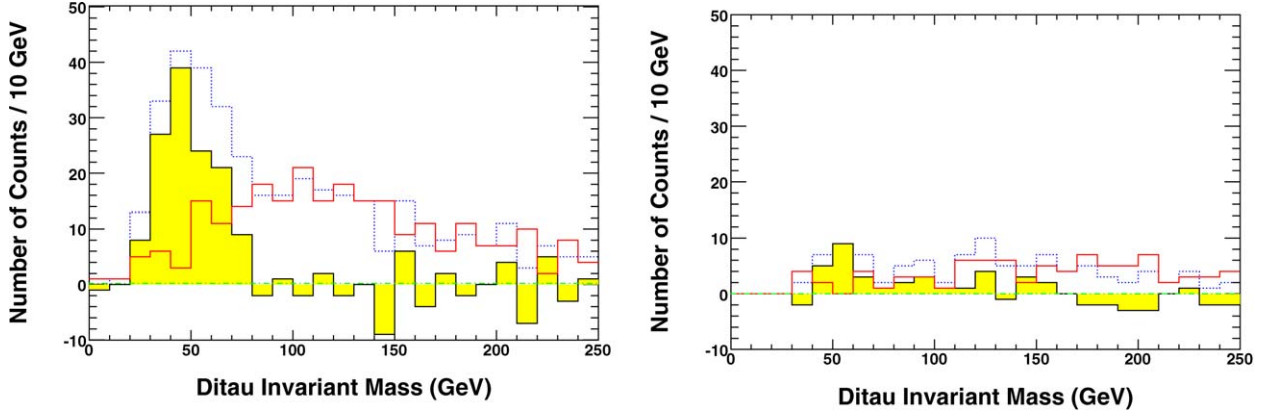


Fig. 5. [Left] Same as in Fig. 4, but using a randomly-selected 10 fb<sup>-1</sup> SUSY sample that is analyzed with  $\epsilon = 50\%$  and  $f_{j \rightarrow \tau} = 1\%$ .  $M_{\tau\tau}^{\max} = 78.7$  GeV can still be inferred and a clear peak is visible. Note that the  $t\bar{t}$  contribution in  $M_{\tau\tau}^{\text{vis}} < 100$  GeV is estimated to be a few OS–LS counts and has not been plotted. [Right] The same sample but requiring all  $\tau$  candidates to have  $p_T^{\text{vis}} > 40$  GeV. The characteristic di-tau mass distribution has disappeared.

150 GeV seen in Fig. 4 becomes statistically insignificant here. The dominant SM backgrounds are events with one jet misidentified as a  $\tau$  and one real  $\tau$  from  $t\bar{t}$  and  $W$  + jets events [22,23]. We still see some cancelation in OS–LS and the di-tau mass distributions are spread over a wide range of the di-tau mass. For example, the number OS–LS counts from  $t\bar{t}$  events that survive our selection cuts is expected to be 6 per 10 fb<sup>-1</sup> for the di-tau mass below 100 GeV and the contribution from  $W$  + jets events also appears to be smaller.<sup>1</sup> These events mostly do not contribute to the OS–LS combination. We do not consider them further. It should be noted that a set of similar kinematical cuts is also used in Ref. [9] and the SM background was also found to be small. To further illustrate the importance of reconstructing  $\tau$ 's with  $p_T^{\text{vis}} \gtrsim 20$  GeV, the RHS of Fig. 5 shows that the mass peak disappears for the same sample, if we require all  $\tau$ 's to be above 40 GeV.

For any coannihilation signal to be established a necessary (but not sufficient) condition is that an excess of signal events above background should be readily observed. Fig. 6 shows the expected yield of OS–LS counts below the end point per 10 fb<sup>-1</sup> as a function of  $\Delta M$ . For comparison, we show the results for  $\epsilon = 50\%$  and  $f_{j \rightarrow \tau} = 1\%$ , along with the ideal  $\tau$  ID condition of  $\epsilon = 100\%$  and  $f_{j \rightarrow \tau} = 0\%$  but scaled down by a factor 4 due to  $1/\epsilon^2$ . It is remarkable to see that there is no significant difference between two cases, suggesting that the counting is very insensitive to the fake rate. This suggests that the counting nearly perfectly reflects the counting of  $\tilde{\chi}_2^0$ 's if one takes into account the  $\tau$  ID efficiency. This also indicates that in the signal region there is only a small contamination from the wrong combination events. Fig. 6 also shows the numbers of OS–LS counts if the gluino mass is varied by approximately  $\pm 5\%$  (and thus

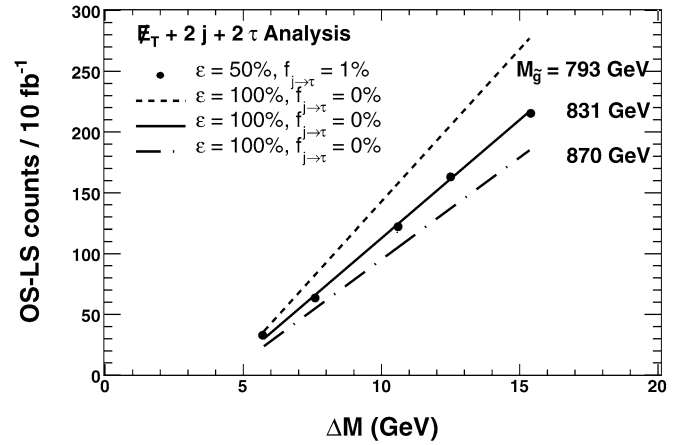


Fig. 6. The mean number of OS–LS counts below the end point per 10 fb<sup>-1</sup> of data as a function of  $\Delta M$ . The solid circles are for  $\epsilon = 50\%$  and  $f_{j \rightarrow \tau} = 1\%$ . The solid line is the case with  $\epsilon = 100\%$  and  $f_{j \rightarrow \tau} = 0\%$ , but with the number of OS–LS counts scaled down by a factor of 4 due to  $1/\epsilon^2$ . The uncertainty of each circle is about its own size based on 200 fb<sup>-1</sup> SUSY MC samples. The dashed and dash-dotted lines are when the gluino masses are varied by about 5%.

also the  $\tilde{\chi}_2^0$  and  $\tilde{\chi}_1^0$  masses), but maintaining the same  $\Delta M$  values. Heavier (lighter) gluino mass is reflected as a smaller (larger) production cross section, thus with a smaller (larger) yield.

We next determine the luminosity necessary to observe OS–LS counts with a  $5\sigma$  significance. We define  $\sigma \equiv (N_{\text{OS}} - N_{\text{LS}})/\sqrt{N_{\text{OS}} + N_{\text{LS}}}$ , again require  $M_{\tau\tau}^{\text{vis}} < M_{\tau\tau}^{\max}$ , and use the results in Fig. 6 to parameterize the number of OS–LS counts as a function of  $\Delta M$ .<sup>3</sup> The luminosity required for as a  $5\sigma$  excess as a function  $\Delta M$  is shown in Fig. 7. We conclude that the characteristic coannihilation signal ( $\Delta M = 5$ –15 GeV) can be detected at the LHC with as few as 3 fb<sup>-1</sup> if  $\Delta M$  is large ( $\simeq 15$  GeV) and with 10 fb<sup>-1</sup> if  $\Delta M$  is small (as-

<sup>1</sup> We accept 115  $t\bar{t}$  and 67  $W(\rightarrow \tau\nu)$  + jet events for 10 fb<sup>-1</sup> in  $\cancel{E}_T + 2$  jet +  $2\tau$  channel with  $\epsilon = 50\%$  and  $f_{j \rightarrow \tau} = 1\%$ . Most of these events are fake-real combinations.

<sup>2</sup> The true end point value ( $M_{\tau\tau}^{\max}$ ) is not known a priori. For a real data, we will find  $M_{\tau\tau}^{\max}$  from the shape in excess. In the present study, we simply use the true value to estimate the required luminosity for a  $5\sigma$  discovery. We also note that  $M_{\tau\tau}^{\max}$  is not used to extract  $\Delta M$ .

<sup>3</sup> In our simulation, we obtain  $N(x, y) = (-8.19 + 1.95x) \cdot y^{-4.62}$ ,  $M_{\tau\tau}^{\text{peak}}(x, y) = (30.3 + 1.96x - 0.0355x^2) \cdot (0.282 + 0.718y)$ , and  $\sigma_M(x) = 3.29 + 1.21x$ . Here  $x = \Delta M$  and  $y = M_{\tilde{g}}/(831.2 \text{ GeV})$ .

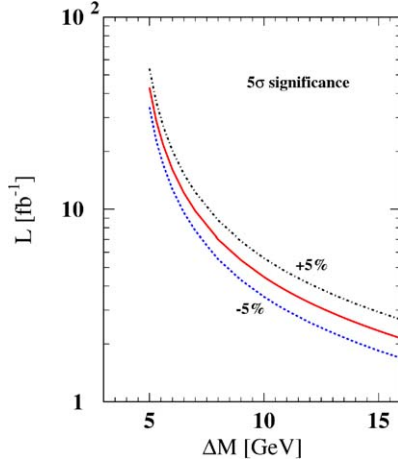


Fig. 7. The luminosity necessary to establish a  $5\sigma$  significance in the number of OS–LS counts for the coannihilation region. The band reflects a variation due to the gluino mass by  $\pm 5\%$  from a nominal gluino mass of 831 GeV in our reference model (see Table 1).

suming the SUSY GUT models are correct and the scale is  $M_{\tilde{g}} = 831$  GeV).

The second criteria we consider to help establish the coannihilation region signal is the observation of  $M_{\tau\tau}^{\text{peak}}$  at the correct location. Within mSUGRA models, since the  $\tilde{g}$ ,  $\tilde{\chi}_1^0$  and  $\tilde{\chi}_2^0$  masses are related,  $M_{\tau\tau}^{\text{max}}$  changes with  $M_{\tilde{\tau}_1}$  for a given  $M_{\tilde{\chi}_1^0}$ . This also means  $M_{\tau\tau}^{\text{peak}}$  changes with  $\Delta M$ . Fig. 8 shows  $M_{\tau\tau}^{\text{peak}}$  as a function of  $\Delta M$ ; any experimental observation would need to be consistent with this small range of 39–52 GeV for the case of  $M_{\tilde{g}} = 831$  GeV.

We next comment on two effects that could change the expected  $M_{\tau\tau}^{\text{peak}}$  value. The first is that since there is a direct relationship between  $M_{\tilde{\chi}_2^0}$  and  $M_{\tilde{g}}$ , from Eq. (1), the peak position is expected to be a function of  $M_{\tilde{g}}$  for a given  $\Delta M$ . If  $M_{\tilde{g}}$  is changed from our nominal value but the  $\Delta M$  value is maintained, we find  $\delta M_{\tau\tau}^{\text{peak}} / M_{\tau\tau}^{\text{peak}} \simeq \delta M_{\tau\tau}^{\text{max}} / M_{\tau\tau}^{\text{max}} = 0.718 \delta M_{\tilde{g}} / M_{\tilde{g}}$ . This is directly observed in Fig. 8 and effectively expands the observation range to 38–54 GeV. We also study the potential impact of varying  $\tau$  ID conditions. On the same figure we show (a)  $\epsilon = 100\%$  and  $f_{j \rightarrow \tau} = 0\%$  and (b)  $\epsilon = 50\%$  and  $f_{j \rightarrow \tau} = 1\%$  and see that there is no systematic peak shift due to the jet  $\rightarrow \tau$  fake rate. This can be explained by the fact that the jet misidentified as a  $\tau$  has no correlation with the  $\tau$  leptons from the  $\tilde{\chi}_2^0$  decay; both OS and LS di-tau mass distributions are affected equally in its shape, and thus will cancel in the difference to good approximation.

As an aside we note that there is a non-coannihilation region where a low energy  $\tau$  lepton is expected when the  $\tilde{\tau}_1$  mass is close to the  $\tilde{\chi}_2^0$  mass instead of the  $\tilde{\chi}_1^0$ . In this “inverted mass” scenario,  $\Delta M_{\text{inv}} \equiv M_{\tilde{\chi}_2^0} - M_{\tilde{\tau}_1} = 5\text{--}15$  GeV. SUSY masses in two particular cases are listed in Table 2, compared to our reference point ( $\Delta M = 10.6$  GeV and  $M_{\tau\tau}^{\text{max}} = 78.7$  GeV). The di-tau mass distribution for the events would look similar to those in the coannihilation region, but we expect a difference in the invariant mass of the jet– $\tau_h$ – $\tau_h$  system in the  $\tilde{q} \rightarrow q\tilde{\chi}_2^0$  decay where the squarks are heavier by about 30 GeV compared

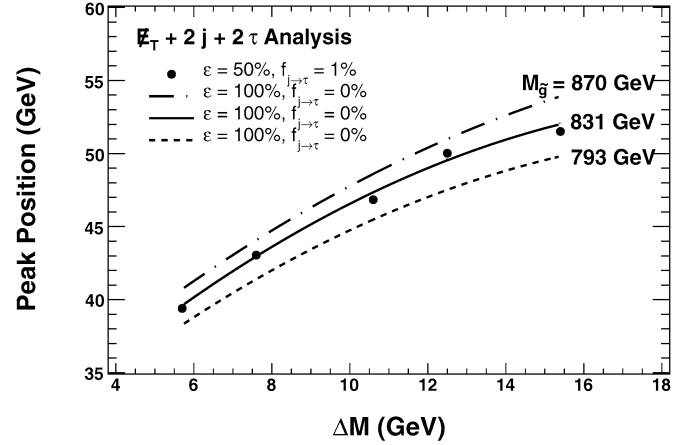


Fig. 8. The peak of the  $M_{\tau\tau}^{\text{vis}}$  distribution as a function of  $\Delta M$ . The solid circles are for  $\epsilon = 50\%$  and  $f_{j \rightarrow \tau} = 1\%$ , compared to the solid line for the case with  $\epsilon = 100\%$  and  $f_{j \rightarrow \tau} = 0\%$ . The statistical uncertainty on each circle is about the size of the circle from  $200 \text{ fb}^{-1}$  SUSY MC samples. The dashed and dash-dotted lines are when the  $\tilde{g}$  masses are varied by about 5% and can be understood as coming from the change in the  $\tilde{\chi}_2^0$  mass for a fixed  $\Delta M$ , since mSUGRA provides a fixed relationship between  $M_{\tilde{g}}$  and  $M_{\tilde{\chi}_2^0}$  (see Eq. (1)). Note that the variation due to the fake rate is negligible.

Table 2

Masses (in GeV) of SUSY particles in two “inverted mass” scenarios for  $m_{1/2} = 360$  GeV,  $\tan \beta = 40$ ,  $\mu > 0$ , and  $A_0 = 0$

$m_0$	323.7	315.2
$\tilde{u}_L$	798	795
$\tilde{t}_1$	598	560
$\tilde{\chi}_2^0$	266.0	266.0
$\tilde{\tau}_1$	255.4	247.8
$\tilde{\chi}_1^0$	144.2	144.2
$\Delta M_{\text{inv}} (\equiv M_{\tilde{\chi}_2^0} - M_{\tilde{\tau}_1})$	10.6	18.2
$M_{\tau\tau}^{\text{max}}$	61.4	78.7

to those of the reference point. A full study is beyond a scope of this study, and we will address this in a future paper. We note, however, that the above two cases do not satisfy the relic density constraint and hence are inconsistent with cosmology. Also, while the small  $\Delta M$  of the coannihilation region is natural for mSUGRA to be consistent with WMAP data [7], the inverted mass scenario further requires an artificial fine tuning to make  $M_{\tilde{\chi}_2^0} - M_{\tilde{\tau}_1}$  small.

Having shown that we can establish a  $5\sigma$  excess and that the peak and end point of di-tau mass distribution are consistent with expectations and only occupy a small region of possible values, we next discuss the prospects for measuring  $\Delta M$  with  $10 \text{ fb}^{-1}$  of data using the peak position of the di-tau mass distribution.

#### 4. Measuring $\Delta M$ using $10 \text{ fb}^{-1}$

The  $\cancel{E}_T + 2 \text{ jet} + 2 \tau$  data set provides an opportunity to make a  $\Delta M$  measurement. Since  $M_{\tau\tau}^{\text{peak}}$  varies with  $\Delta M$ , a measurement of  $M_{\tau\tau}^{\text{peak}}$  combined with a measurement of  $M_{\tilde{g}}$  performed elsewhere allows for a measurement of  $\Delta M$ . It should be noted that from Fig. 8, the peak position varies with  $M_{\tilde{g}}$ . This arises from the mSUGRA relations  $M_{\tilde{g}} \simeq 3.1 M_{\tilde{\chi}_2^0}$  and the fact that

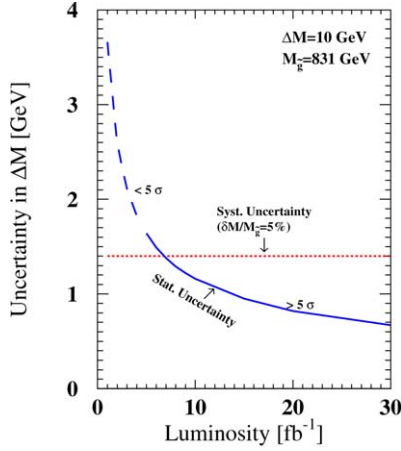


Fig. 9. The uncertainty in the  $\Delta M$  measurement as a function of luminosity. The solid (dashed) curve indicates where this analysis has more than (less than)  $5\sigma$  significance in OS–LS counts and shows the expected statistical uncertainty. We also show the systematic uncertainty (horizontal dotted line) in  $\Delta M$  due to a gluino mass uncertainty of  $\pm 5\%$ .

the gaugino masses enter in the endpoint relation of Eq. (1). We note for completeness that a similar measurement could be done with the results of Fig. 6. This will be done in a separate paper [20].

The statistical uncertainty of the  $\Delta M$  measurement is dominated by the precision of the  $M_{\tau\tau}^{\text{peak}}$  measurement. The statistical uncertainty in the measurement of  $M_{\tau\tau}^{\text{peak}}$  is typically in the 1 GeV range for  $10 \text{ fb}^{-1}$ . Numerically it is given by  $\sigma_M/\sqrt{N}$ , where  $\sigma_M$  is the r.m.s. of the mass distribution (see Fig. 4) and is of the order of 10 GeV, and  $N$  is the number of OS–LS counts in the peak region for a given luminosity (see Fig. 6). For a more detailed parameterizations see footnote 3. The systematic uncertainties due to the uncertainty in the assumed value of  $M_{\tilde{g}}$  changes the  $M_{\tau\tau}^{\text{peak}}$  vs  $\Delta M$  relationship (see Fig. 8). The error is also of the order of 1 GeV for a 5% uncertainty in the gluino mass. The uncertainty due to  $f_{j \rightarrow \tau}$  does not affect the peak measurement.

For the cases of  $\Delta M = 6$  and  $10 \text{ GeV}$ , with  $10 \text{ fb}^{-1}$  of data, we estimate that we can determine the  $\Delta M$  values to be

$$\Delta M = \begin{cases} 6 \pm 1.1^{+1.0}_{-0.9} \text{ GeV} \\ 10 \pm 1.2^{+1.4}_{-1.2} \text{ GeV} \end{cases}$$

where the first uncertainty is due to the statistics and the second due to a gluino mass variation of 5% from the nominal value of 831 GeV. If one assumes a gluino mass uncertainty of 10%, the second uncertainty is almost doubled to  $^{+2.2}_{-1.7}$  and  $^{+3.2}_{-2.3}$  for the 6 and 10 GeV cases, respectively. Fig. 9 illustrates both uncertainties for the  $\Delta M = 10 \text{ GeV}$  case as a function of luminosity. It should be noted that a larger luminosity is required to achieve the same uncertainty for a heavier gluino mass, because the SUSY production cross section is smaller.

## 5. Conclusion

In mSUGRA models, the  $\tilde{\tau}_1 - \tilde{\chi}_1^0$  coannihilation occurs in a large region of parameter space allowed by the relic den-

sity constraint. The characteristic feature of this coannihilation region is a small mass difference ( $\Delta M$ ) between the  $\tilde{\tau}_1$  and the  $\tilde{\chi}_1^0$ . The small mass difference produces final states containing low energy  $\tau$ 's from  $\tilde{\chi}_2^0 \rightarrow \tau \tilde{\tau}_1 \rightarrow \tau \tau \tilde{\chi}_1^0$ . We have demonstrated that if LHC experiments reconstruct/identify  $\tau$ 's with  $p_T > 20 \text{ GeV}$  with an efficiency in the 50% range, we could establish the signal for this coannihilation region using a sample of  $\cancel{E}_T + 2 \text{ jet} + 2\tau$  events. If the  $M_{\tilde{g}}$  were in the 850 GeV range, counting the number of OS–LS di-tau pairs OS–LS di-tau pairs in conjunction with the observation of a mass peak below the expected end points would establish the signal with as few as  $3\text{--}10 \text{ fb}^{-1}$  of data. Larger luminosity would be required to increase  $M_{\tilde{g}}$ . We note that although we have assumed that the jet  $\rightarrow \tau$  fake probability was 1%, our results appear to be insensitive to the fake rate. Using the di-tau mass measurement and assuming that the gluino mass is already measured, we have further shown that a measurement of  $\Delta M$  is possible even with  $10 \text{ fb}^{-1}$  of data. For  $\Delta M = 10 \text{ GeV}$ , the statistical uncertainty is 12%, with a 14% additional uncertainty due to an assumed 5% uncertainty in the gluino mass. Again, the results are insensitive to the fake rate.

We note that the signal of  $\cancel{E}_T + 1 \text{ jet} + 3\tau$  also occurs at a reduced rate from gaugino pairs, but with lower backgrounds. However, it can provide a complementary signal that could help solidify the discovery of the coannihilation signal at the LHC.

The coannihilation region is also present in most non-universal SUGRA models, and an analysis similar to the one here for mSUGRA could be performed for these. The main requirements for an observable signal would be that the  $\tilde{\chi}_2^0$  decays predominantly to  $\tau$ 's, and that the decay of the parent gluinos and squarks to  $\tilde{\chi}_2^0$  is not suppressed.

## Acknowledgements

We thank Kamal Benslama for inspiring us to use final states with two  $\tau$ 's and for technical help throughout this analysis. We also thank Y. Santos for useful discussions. This work is supported in part by a DOE Grant DE-FG02-95ER40917, a NSF Grant PHY-0101015, and in part by NSERC of Canada.

## References

- [1] D.Z. Freedman, P. Van Nieuwenhuisen, S. Ferrara, Phys. Rev. D 13 (1976) 3214.
- [2] S. Deser, B. Zumino, Phys. Lett. B 65 (1976) 369.
- [3] A.H. Chamseddine, R. Arnowitt, P. Nath, Phys. Rev. Lett. 49 (1982) 970.
- [4] R. Barbieri, S. Ferrara, C.A. Savoy, Phys. Lett. B 119 (1982) 343; L. Hall, J. Lykken, S. Weinberg, Phys. Rev. D 27 (1983) 2359; P. Nath, R. Arnowitt, A.H. Chamseddine, Nucl. Phys. B 227 (1983) 121.
- [5] For a review, see P. Nilles, Phys. Rep. 110 (1984) 1.
- [6] J. Ellis, K. Olive, Y. Santos, V. Spanos, Phys. Lett. B 565 (2003) 176; R. Arnowitt, B. Dutta, B. Hu, hep-ph/0310103; H. Baer, C. Balazs, A. Belyaev, T. Krupovnickas, X. Tata, JHEP 0306 (2003) 054; B. Lahanas, D.V. Nanopoulos, Phys. Lett. B 568 (2003) 55; U. Chattopadhyay, A. Corsetti, P. Nath, Phys. Rev. D 68 (2003) 035005; E. Baltz, P. Gondolo, JHEP 0410 (2004) 052; A. Djouadi, M. Drees, J.-L. Kneur, hep-ph/0602001.
- [7] WMAP Collaboration, D.N. Spergel, et al., Astrophys. J. Suppl. 148 (2003) 175.

- [8] H. Baer, A. Belyaev, T. Krupovnickas, J. O’Farrill, JCAP 0408 (2004) 005.
- [9] I. Hinchliffe, F.E. Paige, Phys. Rev. D 61 (2000) 095011.
- [10] F. Heinemann, hep-ex/0406056.
- [11] V. Khotilovich, R. Arnowitt, B. Dutta, T. Kamon, Phys. Lett. B 618 (2005) 182.
- [12] ALEPH, DELPHI, L3, OPAL Collaborations, The LEP Working Group for Higgs Boson Searches, G. Abbiendi, et al., Phys. Lett. B 565 (2003) 61.
- [13] M. Alam, et al., Phys. Rev. Lett. 74 (1995) 2885.
- [14] Particle Data Group, S. Eidelman, et al., Phys. Lett. B 592 (2004) 1.
- [15] Muon  $g - 2$  Collaboration, G. Bennett, et al., Phys. Rev. Lett. 92 (2004) 161802.
- [16] M. Davier, hep-ex/0312065.
- [17] K. Hagiwara, A. Martin, D. Nomura, T. Teubner, Phys. Rev. D 69 (2004) 093003.
- [18] F. Paige, S. Protopescu, H. Baer, X. Tata, hep-ph/0312045. We use ISAJET version 7.63.
- [19] ATLFast is the ATLAS fast simulation package, where the simulation is performed by smearing the MC truth information directly with resolutions measured in full simulation studies. We use version 7.0.2, see <http://www.hep.ucl.ac.uk/atlas/atlfast/>.
- [20] R. Arnowitt, A. Aurisaro, B. Dutta, T. Kamon, N. Kolev, P. Simeon, D. To-back, P. Wagner, in preparation.
- [21] CDF Collaboration, D. Acosta, et al., Phys. Rev. Lett. 95 (2005) 131801. The jet  $\rightarrow \tau$  fake probability ( $f_{j \rightarrow \tau}$ ) is measured to be 1.1% ( $E_{\text{jet}} \simeq 20$  GeV) down to 0.2% ( $E_{\text{jet}} \gtrsim 100$  GeV) as a function of the jet energy. We simply assume a constant value (= 1%) for our simulation study.
- [22] H. Baer, C.H. Chen, F. Paige, X. Tata, Phys. Rev. D 52 (1995) 2746.
- [23] I. Hinchliffe, F.E. Paige, M.D. Shapiro, J. Soderqvist, W. Yao, Phys. Rev. D 55 (1997) 5520.